Review of Scientific Instruments

RESEARCH ARTICLE | MARCH 18 2025

Tunable accordion optical lattice for precise control of Rydberg atom interactions in magneto-optical traps (MOTs)

Hao Zhang ; Ying Miao ; Yifei Cao ; Xue Liang ; Mingyong Jing ; Linjie Zhang

Rev. Sci. Instrum. 96, 033201 (2025)
https://doi.org/10.1063/5.0253391

Review of Scientific Instruments ARTICLE pubs.aip.org/aip/rsi

Tunable accordion optical lattice for precise control of Rydberg atom interactions in magneto-optical traps (MOTs)

Cite as: Rev. Sci. Instrum. 96, 033201 (2025); doi: 10.1063/5.0253391
Submitted: 16 December 2024 • Accepted: 21 February 2025 •
Published Online: 18 March 2025

Hao Zhang,[1,2,a] Ying Miao,[1,2] Yifei Cao,[1,2] Xue Liang,[1,2] Mingyong Jing,[1,2] and Linjie Zhang[1,2]

AFFILIATIONS

[1] State Key Laboratory of Quantum Optics Technologies and Devices, Institute of Laser Spectroscopy, Shanxi University, Taiyuan, Shanxi 030006, China
[2] Collaborative Innovation Center of Extreme Optics, Shanxi 030006, China

[a] **Author to whom correspondence should be addressed:** haozhang@sxu.edu.cn

ABSTRACT

Precise control of Rydberg atom interactions in magneto-optical traps is essential for advanced quantum technologies, yet fine-tuning of strong Rydberg interactions remains challenging. To address this, we present a tunable accordion optical lattice with dynamically adjustable lattice spacings. By stabilizing power and polarization, we improve the power stability of the device by 56.53%, achieving lattice spacings ranging from 46.63 to 2.58 μm and generating stable interference patterns consistent with theoretical predictions. The lattice's versatility and precision enable control of atomic interactions, supporting simulations of quantum phase transitions and many-body physics while advancing quantum simulations and information processing.

I. INTRODUCTION

Quantum simulation has been a universal and efficient tool for investigating complex many-body systems that are otherwise intractable through analytical calculations or numerical simulations. Ultracold atomic systems have emerged as highly versatile platforms for quantum simulations due to their ability to regulate key parameters, such as the precise tuning of interaction strength and spatial configurations.[1,2] Rydberg atoms are particularly prominent candidates for quantum simulations for their exaggerated properties in terms of strong long-range interactions that scale with the n^7 dependence of the principal quantum number.[3,4] Interactions between Rydberg atoms can be tuned on a large scale in various ways, including the application of external electric fields, access to different states, and control of atomic density. This tunability makes Rydberg atoms a powerful tool for simulating quantum phase transitions, topological matter, and non-equilibrium dynamics.[5,6]

Optical lattices[7] provide a robust platform for quantum simulations by enabling precise control over the atomic positions and tunneling rates, thereby facilitating the exploration of exotic quantum states.[8,9] Recent experimental implementations of accordion optical lattices, such as those demonstrated by Wang *et al.*[10] have shown great potential for realizing highly controllable Rydberg arrays and probing interaction-driven phase transitions with fine control over atomic spacing. These advances highlight the enormous possibilities that quantum simulators based on optical lattices bring to the field of many-body physics and quantum simulation.[11,12]

The long-range interactions between Rydberg atoms are governed by distance-dependent potentials, typically characterized by C_6/r^6 dependence for van der Waals interactions and C_3/r^3 for resonant dipole–dipole interactions.[13,14] These interaction potentials can be modulated by controlling the interatomic separation, enabling the tunability of interaction strengths in a wide range of several orders of magnitude. Recent experimental results have demonstrated the ability to precisely control Rydberg interactions in ultracold atomic ensembles, where interatomic distances are finely tuned using optical tweezers or adjustable optical lattices.[15,16] Studies by Schau *et al.*[17] and Zeiher *et al.*[18] have shown the feasibility precise control of atomic interactions in the simulation of correlated many-body quantum systems and the realization of novel quantum phases. The flexibility in tuning interaction strengths and the

strong interaction effects of Rydberg atoms make them a potential platform for exploring exotic quantum states[19] and non-trivial topological phenomena.[20] To take full advantage of the tunability of distance-dependent Rydberg interactions, it is essential to design experimental apparatus that enable the preparation of specific atomic states and configurations.

This work demonstrates the construction and experimental optimization of a tunable accordion optical lattice for precise control of Rydberg interactions. This flexible lattice configuration enables fine adjustments to lattice constants with high spatial precision,[10] providing control over atomic spacing and interaction potentials between trapped Rydberg atoms. By tuning the lattice constant, interaction strengths can be accurately regulated, allowing for the preparation of specific quantum states with sub-wavelength precision. This capability is critical for studying distance-dependent interactions and their impact on quantum many-body dynamics.[21–23]

II. STRONG RYDBERG INTERACTIONS

Rydberg atoms are particularly remarkable for their extremely strong long-range interactions, which take the form of the van der Waals potential: $V_{vdW} = \frac{C_6}{R^6}$ and these interactions are orders of magnitude stronger than those observed between atoms in their ground state. The dispersion coefficient[24] given by $C_6 = \sum_{r'r''} \frac{|\langle r'r''|V(R)|rr\rangle|^2}{\Delta_{r'r''}}$ is in proportion of n^{11} (n is principal quantum number), R is the interatomic distance, and $V(R)$ is the interaction potential. The states $|rr\rangle$ and $|r'r''\rangle$ are dipole-coupled pair states, and $\Delta_{r'r''}$ is the energy gap between these two pair states. Considering the van der Waals interactions, atoms in P and D states are assumed to be aligned parallel to each other. The strong interactions make Rydberg atoms an ideal platform for studying strongly correlated quantum systems.[25]

The strong long-range interactions between Rydberg atoms would induce a novel quantum phenomenon known as the Rydberg blockade effect.[26] This effect creates a blockade region around an excited atom, within which only one Rydberg atom can be excited. The blockade radius,[27,28] R_b, which defines this region, can be expressed as $R_b = (C_6/\gamma_L)^{\frac{1}{6}}$, where γ_L is the laser linewidth.

Within the blockade region, the atoms are indistinguishable, and the excitation becomes delocalized across the ensemble, leading to a quantum superposition state.[5]

In our study, ^{133}Cs atoms are trapped and cooled in a magneto-optical trap (MOT).[29,30] The goal is to predict and experimentally observe the blockade effect, which prevents multiple excitations within a characteristic region known as the blockade radius.

Figure 1 shows the dependencies of C_6 and the blockade radius on the principal quantum number n, where $\gamma_L = 0.1$ kHz, in accordance with our experimental setup. The gray shaded area represents the range over which the blockade radius can be experimentally tuned. The detailed results are provided in Table I.

To experimentally utilize the blockade effect, precise control over interatomic distances is essential, motivating the need for adjustable lattice setups. Modulation of laser frequency and intensity is a crucial method for controlling atomic quantum states and interactions. Adjusting the laser frequency can modify atomic interactions by shifting the atomic resonance. In particular, changes in frequency and intensity can change the atomic potential in the optical lattice,[31] thereby tuning the interaction strength. Higher atomic densities reduce the average atomic spacing, enhancing atomic interactions, while lower atomic densities increase the spacing and weaken interactions. Although precise regulation of interactions is challenging in many optical lattices, the accordion optical lattice employed in our setup achieves this by allowing position adjustments, enabling fine-tuned control over atomic interactions.[11]

III. OPTICAL EXPERIMENTAL SETUP

An accordion optical lattice[32,33] as the name suggests, is an optical lattice whose lattice spacing[34] can be varied within a certain range by adjusting the wavelength of the lattice laser or the angles between two interference laser beams. In this work, we adopted the latter

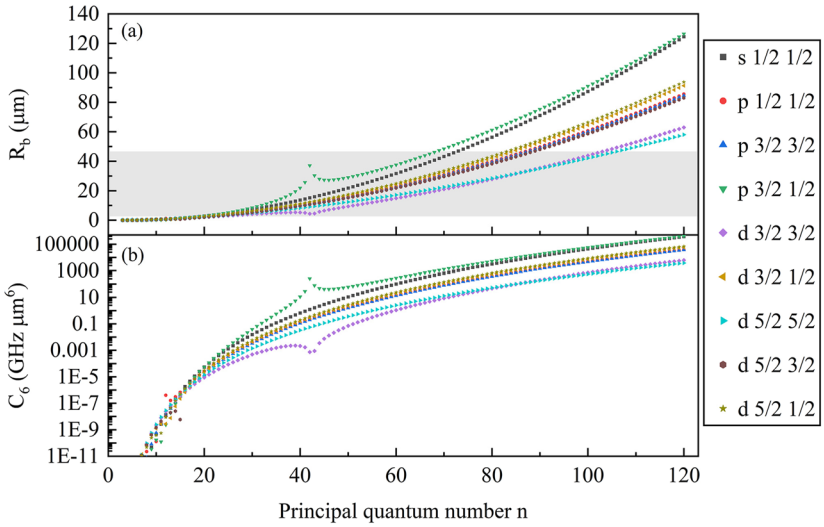

FIG. 1. Panels (a) and (b) show the blockade radius and C_6 coefficient as functions of the principal quantum number n for the excitation of ^{133}Cs from the $nS_{1/2}$ to $nD_{5/2}$ state, with $\gamma_L = 0.1$ kHz. The gray shaded area represents the tunable range for strong interactions, where the blockade radius can be adjusted between 46.63 and 2.58 μm.

TABLE I. Blockade radius R_b is calculated using the van der Waals potential model.

n	State	$\lvert m_j\rvert$	R_b (μm)
20–72	$S_{1/2}$	1/2	2.85–45.69
21–87	$P_{1/2}$	1/2	2.79–46.62
21–87	$P_{3/2}$	3/2	2.66–45.98
20–68	$P_{3/2}$	1/2	2.85–46.14
23–103	$D_{3/2}$	3/2	2.68–46.51
21–84	$D_{3/2}$	1/2	2.71–46.30
22–106	$D_{5/2}$	5/2	3.49–46.63
22–88	$D_{5/2}$	3/2	3.53–45.96
20–83	$D_{5/2}$	1/2	3.52–46.54

method. As shown in Fig. 2, the setup includes a half-wave plate (HWP), a quarter-wave plate (QWP), two polarizing beam splitters (PBS), a 0° reflecting mirror, an aspherical lens with the focal length of 150 mm, and a Raspberry Pi camera. The entire device is assembled using a 30 and 60 mm optical cage system, which provides an efficient way for quick and precise optical alignment.

Two motorized translation stages (MTS, M30X/M) are used to hold a pair of PBS and the aspherical lens, enabling precise control of the intersection angle between the two laser beams. The variation of the intersection angle is mainly achieved by adjusting the positions of the PBS along the z axis using the MTS, with the step size set to 1 mm. The aspherical lens is finely tuned to compensate for displacement deviations, ensuring precise alignment. This configuration enables the generation of stable and bright interference patterns. The lattice spacing s is expressed as

$$s = \frac{\lambda}{2d\,\sin\,\theta} = \frac{\lambda}{2}\sqrt{1+\left(\frac{f_F}{d}\right)^2}, \tag{1}$$

where λ is the laser wavelength, θ is half the angle between two laser beams, f_F is the focus length of lens, and d is half the distance between two beams.

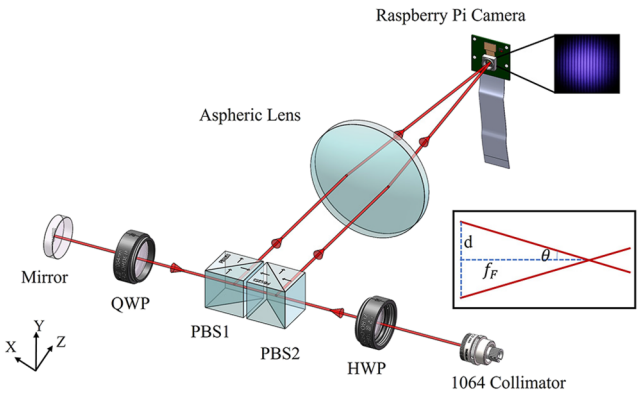

FIG. 2. Schematic of the experimental setup for generating the accordion optical lattice. The setup includes the HWP, QWP, two PBS, Mirror, aspherical lens (focal length is 150 mm), and a Raspberry Pi camera.

IV. RESULTS AND STABILITY

In this section, the experimental results are presented. The stability of the interference pattern and the intersection angle are evaluated using both simulation and experimental data. We then analyze the results following power stabilization to assess the stability and contrast of the interference fringes.

The intensity profiles of the interference patterns at various intersection angles were captured using a camera equipped with pixel sensors sensitive to red, green, and blue color channels. Notably, the blue-sensitive pixels, with a pixel size of 1.12 μm, exhibited the highest contrast in the interference patterns, as shown in Figs. 3(c)–3(f), making them optimal for further high-resolution measurements. Correspondingly, the measured lattice spacing as a function of laser intersection angle is presented in Fig. 4. Although the measured spacing is constrained by the physical dimensions of the optical components, it ranges from 46.63 to 2.58 μm, which is in excellent agreement with the theoretical fit derived from Eq. (1).

Achieving precise measurements requires highly stable experimental conditions, particularly in terms of power and polarization. Stability in these parameters is crucial for the efficiency of atomic capture in a MOT and for maintaining the fidelity of atomic populations, which would be influenced by fluctuations either of power or polarization. These fluctuations would directly lead to the instabilities of the lattice potential and further the number of trapped atoms in the lattice. Consistent experimental conditions are essential to ensure reproducibility, as instability in power or polarization increases system noise, causing fluctuations in atomic capture and reducing the overall fidelity of the experiment. These improvements are critical for achieving reliable control of atomic interactions in quantum simulations.

To address these challenges, we optimized the beam setup by implementing power and polarization stabilization. Power stabilization was achieved using an acousto-optic modulator (AOM), which effectively minimized power fluctuations and ensured consistent experimental results. Polarization stabilization was accomplished with employing polarization components, such as a HWP and a QWP, which precisely adjusted and stabilized the laser's polarization direction and ellipticity, thereby maintaining a linearly polarized laser beams essential for lattice generation.

Figure 5 illustrates the long-term stability of the system. Panel (a) shows the power fluctuation, with the black curve representing the free-running power, which has a relative standard deviation of 1.302%. Following the implementation of power and polarization stabilization, the relative standard deviation is reduced to 0.566%, reflecting a significant improvement of 56.53% in stability. The inset plots display the corresponding Allan variance. Panel (c) shows the fringes contrast as a function of the spacing and intersection angle. The axes of lattice spacing and intersection angle are not linear, and the error of fringes contrast increases as the lattice spacing reduces or the intersection angle grows, primarily due to the limited pixel resolution of the Raspberry Pi camera. This limitation becomes more evident at smaller spacing, where finer fringe patterns reduced the accuracy of contrast measurements. A higher-resolution camera could reduce this error. In addition, a larger range of lattice spacing could be achieved by selecting optics components with larger dimensions.

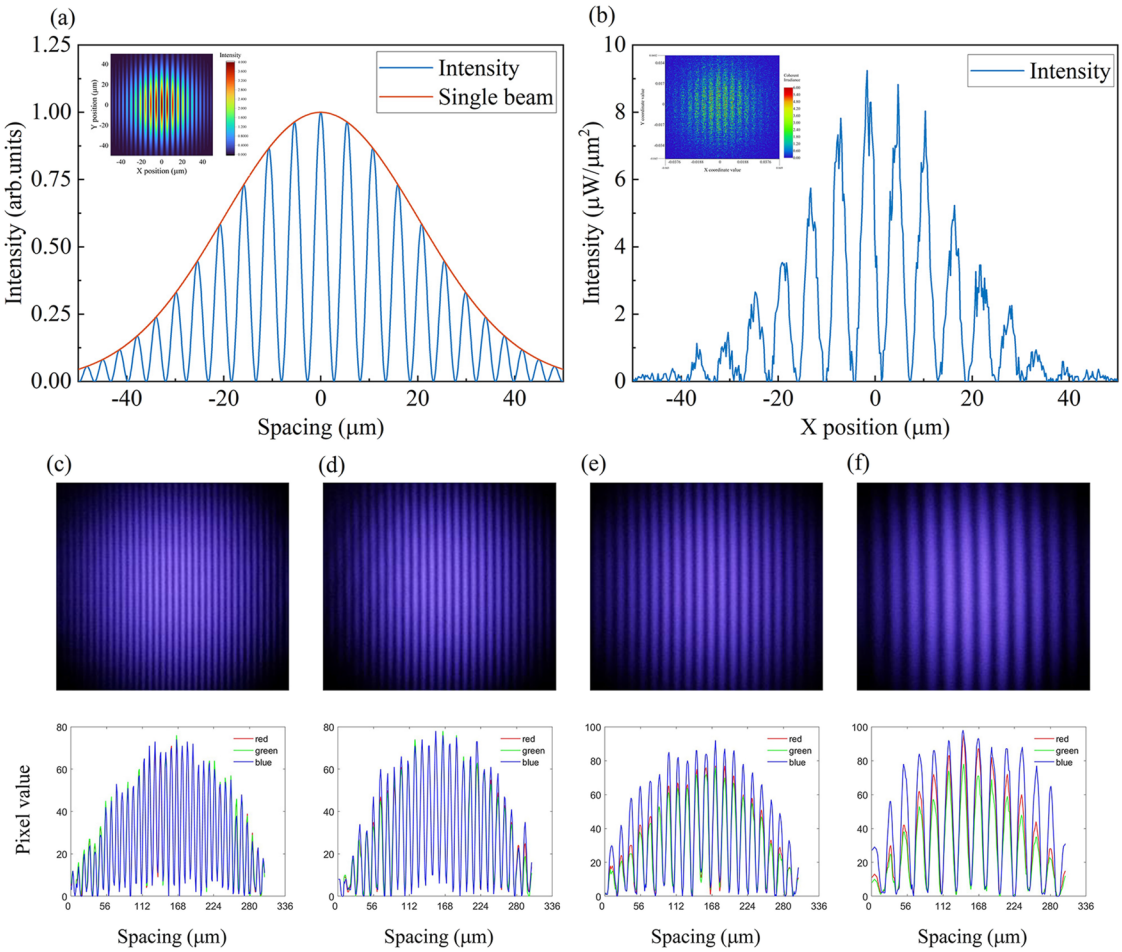

FIG. 3. (a)(b) Interference patterns and cross-sectional analysis for a beam angle of 10.11°, corresponding to a fringe spacing of 6.7 μm. The simulation (Zemax) predicts a fringe spacing of 6.5 μm, demonstrating good agreement with experimental data. Figures (c)–(f) display the experimental interference patterns along with the corresponding data.

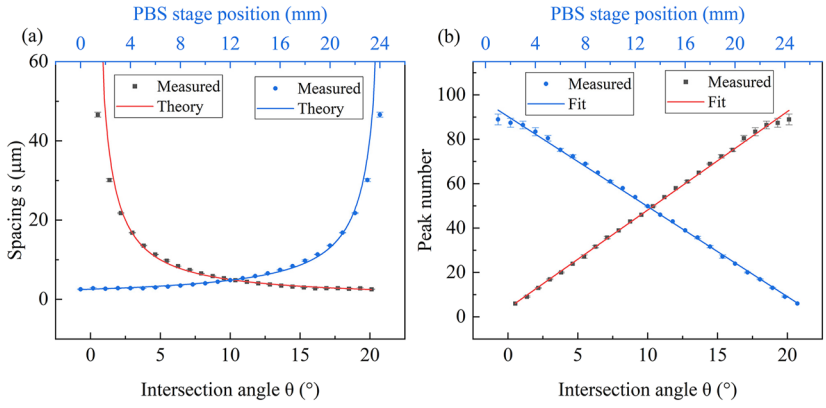

FIG. 4. Measured lattice spacing (a) and peak numbers (b) as functions of the intersection angle θ and the PBS stage position. The measured values are fitted to Eq. (1), showing good agreement with theoretical expectations.

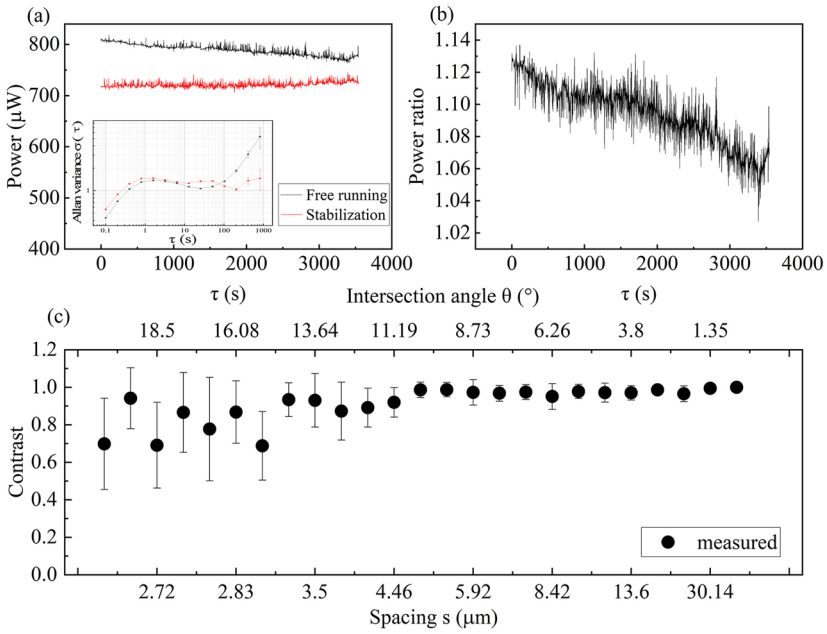

FIG. 5. This figure illustrates the long-term stability characteristics of the system. Panel (a) shows the power variations of the system under both free-running and stabilization conditions, with the inset plots displaying the corresponding Allan variance results. Panel (b) depicts the power ratio under free-running and stabilization conditions. Panel (c) shows the contrast as a function of the spacing and intersection angle.

V. LATTICE POTENTIAL AND TRAPPING ANALYSIS

Understanding the lattice potential and trapping parameters is crucial for fine-tuning the confinement and interaction properties of ultracold atoms, enabling precise control for strong Rydberg interactions. An accordion optical lattice is a modulated standing wave potential generated by the interference of two laser beams. In our experiment, we analyzed the theory of the optical lattice, estimating key parameters such as the optical lattice potential, trapping frequency, and the Lamb–Dicke parameter (η). When the detuning between the optical field frequency and the atomic transition energy significantly exceeds the Rabi frequency, electronic transitions are suppressed, and the optical field induces perturbations in the atomic energy levels.[35] In this regime, the optical field shifts the atomic energy levels without inducing transitions, as described by the atom's dipole polarizability:[36] $\alpha_i = \frac{2|d|^2}{\hbar}\frac{\omega_i}{\omega_i^2-\omega^2}$, and the corresponding frequency shift is given by $\Delta\omega_s = \frac{\Omega^2}{\omega_i}2(\omega^2-\omega_i^2)$, where ω_i is the atomic transition frequency, ω is the laser angular frequency, d is the dipole moment, and Ω is the laser Rabi frequency. In this context, the interaction with the optical field results in an interaction energy, $U = \vec{d}\cdot\vec{E}$, where $\vec{E}$ is the electric field of light.

Optical lattices use the dipole force exerted by a 1064 nm laser to trapped ultracold atoms in a periodic potential. The depth of the potential can be calculated using

$$U = \hbar\Delta\omega_s = -\frac{\alpha_i}{4}E_0^2. \tag{2}$$

The optical lattice potentials can be further characterized by the trapping frequencies along the axial (z) and radial (r) directions. The axial trapping frequency υ_z is given by $\upsilon_z = \frac{1}{2\pi}\sqrt{\frac{2Uk^2}{m}}$, where k is the lattice wave vector and m is the mass of the atom. The radial trapping frequency υ_r is given by $\upsilon_r = \frac{1}{\pi\omega_0}\sqrt{\frac{U}{m}}$, where ω_0 is the laser waist radius. The Lamb–Dicke parameter is defined to characterize the strength of an optical lattice potential in relation to the atomic recoil energy,[37]

$$\eta = kx_0 = k\sqrt{\frac{\hbar}{2m\omega}}. \tag{3}$$

The trapping angular frequency is given by $\omega = 2\pi\upsilon$; the recoil frequency is $\omega_r = \frac{\hbar k^2}{2m}$; $\vec{k}$ is the wave vector of the probing laser; and x_0 is atomic trap range. When $\eta \ll 1$, the atom is strongly localized within the potential entering the Lamb–Dicke regime, where the recoil frequency is much smaller than the trapping frequency. These frequencies determine the strength of confinement in the optical lattice. In this regime, the atoms are tightly confined, and the recoil frequency shift is effectively absorbed by the optical lattice trapping potential, thereby suppressing sideband excitation.

Table II summarizes the parameters used to calculate the potential depths for various atomic species (^{133}Cs, ^{87}Rb, and ^{23}Na) trapped in the optical lattice, along with their corresponding trapping frequencies and Lamb–Dicke parameters. This configuration significantly enhances the ability to distinguish trapped atoms, providing improved confinement and precise control. Based on theoretical calculations, with a beam power of 20 W and a beam waist of 150 μm, the optical lattice potential depth for the trapped ^{133}Cs atom is estimated to be 178.152 μK. The axial and radial trapping frequencies are calculated as υ_z = 140.318 kHz and υ_r = 224.027 Hz, respectively. The Lamb–Dicke parameters, $\eta_z = 0.304 < 1$ and $\eta_r = 7.613 > 1$, indicate that the optical lattice is well-suited for effective atom trapping, providing a solid foundation for achieving the anticipated experimental outcomes. In addition, the table provides a practical reference for determining the optimal laser power and beam waist for the 1064 nm laser used in the experiment.

TABLE II. Theoretical parameters for the lattice potentials of ^{133}Cs, ^{87}Rb, and ^{23}Na atoms, calculated for a beam power of 20 W and a beam waist of 150 μm.

Parameter	^{133}Cs	^{87}Rb	^{23}Na	Units
α_i	1.154×10^{-38}	7.277×10^{-39}	2.546×10^{-39}	$(\mathrm{C\,m^2})/\mathrm{V}$
U	2.460×10^{-27}	1.551×10^{-27}	5.429×10^{-28}	J
U/k_B	178.152	112.369	39.320	μK
U/E_R	1796.491	620.894	32.769	E_R
υ_z	140.318	137.810	158.500	kHz
υ_r	224.027	220.022	253.055	Hz
η_z	0.304	0.415	0.996	<1
η_r	7.613	10.377	24.916	>1

VI. CONCLUSION

In this paper, we present an experiment involving a tunable accordion optical lattice to achieve precise control of Rydberg atom interactions in a magneto-optical trap (MOT), based on the theory of strong Rydberg interactions. Our results demonstrate the significant advantages of tunable accordion optical lattices in achieving high precision and stability for atomic manipulation. By implementing power and polarization stabilization, we improved the device's power stability by 56.53%. This enhancement enabled lattice spacings ranging from 46.63 to 2.58 μm, producing stable interference patterns that correspond closely to theoretical predictions. In addition, employing a high-resolution camera could further reduce fringe contrast errors, and a wider range of lattice spacings could be achieved by selecting optical components with larger dimensions. The systematic parameterization of equations allows for precise calculations of the optical lattice power and beam waist, offering a strong theoretical basis for different experimental setups. This system's versatility provides a robust foundation for further experimental investigations, particularly in quantum simulations and quantum information processing. These advancements are expected to significantly contribute to the development of quantum technologies and provide novel approaches for exploring many-body physics. Future efforts will focus on using this setup to simulate quantum phase transitions and implementing quantum logic operations.

ACKNOWLEDGMENTS

This research is funded by the National Key R&D Program of China (Grant No. 2022YFA1404003), the National Natural Science Foundation of China (Grant Nos. 12104279 and 61827824), the Innovation Program for Quantum Science and Technology (Grant No. 2021ZD0302100), the Shanxi Provincial Key R&D Program (Grant No. 202102150101001), and the Fund for Shanxi "1331 Project" Key Subjects Construction, Bairen Project of Shanxi Province, China.

AUTHOR DECLARATIONS

Conflict of Interest

The authors have no conflicts to disclose.

Author Contributions

Z.H. proposed the project, developed the research. Y.M. and X.L. performed the experiments. Y.M. and H.Z. analyzed the data and prepared the paper. H.Z. and L.Z. supervised the experiment. All authors contributed to discussions of the results and the manuscript and provided revisions of manuscript.

Hao Zhang: Conceptualization (equal); Funding acquisition (equal); Investigation (equal); Methodology (equal); Supervision (equal); Writing – review & editing (equal). **Ying Miao**: Data curation (equal); Formal analysis (equal); Investigation (equal); Writing – original draft (lead). **Yifei Cao**: Data curation (supporting); Investigation (supporting); Methodology (supporting). **Xue Liang**: Data curation (supporting). **Mingyong Jing**: Conceptualization (equal); Supervision (supporting). **Linjie Zhang**: Conceptualization (equal); Supervision (equal).

DATA AVAILABILITY

The data that support the findings of this study are not publicly available at this time within the article but can be obtained from the corresponding author upon reasonable request.

REFERENCES

[1] I. Bloch, Nat. Phys. **1**, 23 (2005).
[2] Y. Wang, Y. Li, J. Wu, W. Liu, J. Hu, J. Ma, L. Xiao, and S. Jia, Opt. Express **29**, 13960 (2021).
[3] K. Singer, J. Stanojevic, M. Weidemüller, and R. Côté, J. Phys. B: At., Mol. Opt. Phys. **38**, S295 (2005).
[4] T. F. Gallagher, *Rydberg Atoms*, *Cambridge Monographs on Atomic, Molecular and Chemical Physics* (Cambridge University Press, 1994).
[5] M. Saffman, T. G. Walker, and K. Mølmer, Rev. Mod. Phys. **82**, 2313 (2010).
[6] D. Jaksch, J. I. Cirac, P. Zoller, S. L. Rolston, R. Côté, and M. D. Lukin, Phys. Rev. Lett. **85**, 2208 (2000).
[7] C. Gross and I. Bloch, Science **357**, 995 (2017).
[8] I. Bloch, J. Dalibard, and W. Zwerger, Rev. Mod. Phys. **80**, 885 (2008).
[9] M. Greiner, O. Mandel, T. W. Hänsch, and I. Bloch, Nature **419**, 51 (2002).
[10] L. Wang, K. Wen, F. Liu, Y. Li, P. Wang, L. Huang, L. Chen, W. Han, Z. Meng, and J. Zhang, Chin. Phys. B **31**, 103401 (2022).
[11] A. Browaeys and T. Lahaye, Nat. Phys. **16**, 132 (2020).
[12] R. S. Watson and J. J. McFerran, J. Opt. Soc. Am. B **38**, 36 (2021).
[13] M. Robinson, B. L. Tolra, M. W. Noel, T. Gallagher, and P. Pillet, Phys. Rev. Lett. **85**, 4466 (2000).
[14] H. Gorniaczyk, C. Tresp, J. Schmidt, H. Fedder, and S. Hofferberth, Phys. Rev. Lett. **113**, 053601 (2014).
[15] Y. Dudin, L. Li, F. Bariani, and A. Kuzmich, Nat. Phys. **8**, 790 (2012).
[16] Z. Meng, L. Wang, W. Han, F. Liu, K. Wen, C. Gao, P. Wang, C. Chin, and J. Zhang, Nature **615**, 231 (2023).
[17] P. Schauß, J. Zeiher, T. Fukuhara, S. Hild, M. Cheneau, T. Macrì, T. Pohl, I. Bloch, and C. Groß, Science **347**, 1455 (2015).
[18] J. Zeiher, R. van Bijnen, P. Schauß, S. Hild, J.-y. Choi, T. Pohl, I. Bloch, and C. Gross, Nat. Phys. **12**, 1095 (2016).
[19] R. Samajdar, D. G. Joshi, Y. Teng, and S. Sachdev, Phys. Rev. Lett. **130**, 043601 (2023).
[20] S. de Léséleuc, V. Lienhard, P. Scholl, D. Barredo, S. Weber, N. Lang, H. Büchler, T. Lahaye, and A. Browaeys, "Observation of a symmetry-protected topological phase of interacting bosons with Rydberg atoms," Science **365**, 775–780 (2019).
[21] A. Schwarzkopf, R. Sapiro, and G. Raithel, Phys. Rev. Lett. **107**, 103001 (2011).
[22] H. Weimer, M. Müller, I. Lesanovsky, P. Zoller, and H. P. Büchler, Nat. Phys. **6**, 382 (2010).

[23]M. D. Lukin, M. Fleischhauer, R. Cote, L. Duan, D. Jaksch, J. I. Cirac, and P. Zoller, Phys. Rev. Lett. **87**, 037901 (2001).
[24]L. Béguin, A. Vernier, R. Chicireanu, T. Lahaye, and A. Browaeys, Phys. Rev. Lett. **110**, 263201 (2013).
[25]D. Tong, S. Farooqi, J. Stanojevic, S. Krishnan, Y. Zhang, R. Côté, E. Eyler, and P. Gould, Phys. Rev. Lett. **93**, 063001 (2004).
[26]M. Müller, A. Kölle, R. Löw, T. Pfau, T. Calarco, and S. Montangero, Phys. Rev. A **87**, 053412 (2013).
[27]K. S. Kleinbach, "Ions and electrons interacting with ultracold atoms: Novel approaches based on Rydberg excitations," Ph.D. thesis, University of Stuttgart, 2018.
[28]A. Micheli, G. K. Brennen, and P. Zoller, Nat. Phys. **2**, 341 (2006).
[29]H. J. Metcalf and P. Van der Straten, *Laser Cooling and Trapping* (Springer Science & Business Media, 1999).
[30]W. Ketterle and N. V. Druten, *Advances in Atomic, Molecular, and Optical Physics* (Elsevier, 1996), Vol. 37, pp. 181–236.
[31]L. H. Kendrick, "An optical accordion trap for two-dimensional ultracold gases of ^{6}Li and ^{23}Na," Ph.D. thesis, Massachusetts Institute of Technology, 2019.
[32]L. Fallani, C. Fort, J. E. Lye, and M. Inguscio, Opt. Express **13**, 4303 (2005).
[33]C. Dietrich, "An accordion-type lattice: A tuneable dipole trap for ultracold gases," Ph.D. thesis, University of Stuttgart, 2018.
[34]J. Ville, T. Bienaimé, R. Saint-Jalm, L. Corman, M. Aidelsburger, L. Chomaz, K. Kleinlein, D. Perconte, S. Nascimbène, J. Dalibard *et al.*, Phys. Rev. A **95**, 013632 (2017).
[35]J. H. Huckans, "Optical lattices and quantum degenerate ^{87}Rb in reduced dimensions," Ph.D. thesis, University of Maryland, 2006.
[36]E. J. Robertson, N. Šibalić, R. M. Potvliege, and M. P. Jones, Comput. Phys. Commun. **261**, 107814 (2021).
[37]T. Xiao, "Experimental study on loading ^{88}Sr into an optical lattice and probing its clock transition," Ph.D. thesis, Chinese Academy of Sciences (National Time Service Center), 2015.